

# NUMERICAL STUDY ON ELECTRON BEAM PROPERTIES IN TRIODE TYPE THERMIONIC RF GUN

K. Mishima, K. Torgasin, K. Masuda, M. Inukai, K. Okumura, H. Negm, M. Omer,  
K. Yoshida, H. Zen, T. Kii, H. Ohgaki

Institute of Advanced Energy, Kyoto University, Gokasho, Uji, Kyoto, 611-0011, Japan

## Abstract

The KU-FEL(Kyoto University- Free Electron Laser) facility uses a thermionic 4.5 cell S-band RF gun for electron beam generation. The main disadvantage of using a thermionic RF gun is the back-bombardment effect, which causes energy drop in the macro pulse. A modification of the thermionic RF gun to a triode type RF gun shall reduce the back-bombardment power and enlarge the macro pulse duration.

In this work we report the results of numerical studies of operational parameters depending on electron beam properties for a triode type thermionic RF.

## INTRODUCTION

A 4.5 cell thermionic RF gun is used as the injector for oscillator type MIR-FEL facility (KU-FEL: Kyoto University Free Electron Laser) at Institute of Advanced Energy, Kyoto University. As compared with photocathode RF gun a thermionic RF gun has advantage of compact and economic structure, easy operation and high averaged current. The disadvantage however is the occurrence of back-bombardment effect. Thereby some electrons are getting into the decelerating phase of the driving RF wave and are accelerated back into the cathode. The back streaming electrons heat up the cathode additionally and the current rises as the consequence. The ramped current leads to limitation of the macro pulse duration. In order to solve this problem and to obtain electron beam of high brightness with long macro pulse duration, which is essential for oscillator type FEL, we are developing what we call a triode type thermionic RF gun [1]. For it an additional small coaxial cavity (triode cavity, hereafter) which serves as a control grid should be attached to the currently used thermionic RF gun. The triode cavity has a separate from the 4.5 cell gun power supply with amplitude and phase controlled with respect to those driving the gun main cavities. Figure 1 shows schematic drawing for the triode RF gun system, where the triode cavity is integrated into the main thermionic RF gun. The thermionic cathode material is located on the inner rod of the triode cavity. The triode cavity geometry and corresponding cavity voltage and cathode emission current were designed for reduction of back-bombardment power by more than 80% [2].

The triode cavity was designed and fabricated, such that experimental proof-of-concept is planned for near future [3].

## COAXIAL CAVITY DESIGN

Figure 2 shows a cross sectional view and a photograph of the triode cavity. An accessible structure with a demountable aperture as shown in the future has an advantage of being able to align and to measure the cathode position.

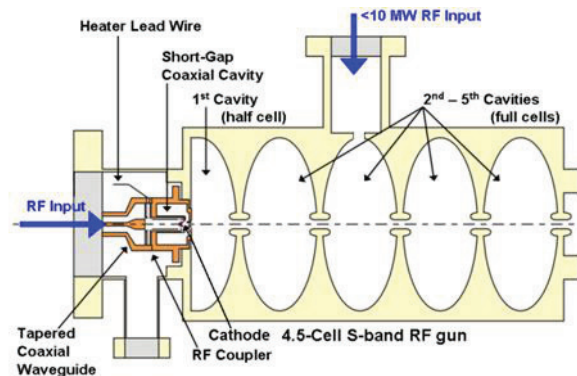


Figure 1: Triode type thermionic RF gun consisting of a small coaxial cavity and the 4.5 cell thermionic RF gun.

The cavity has a stub and spacer tuning system for resonance frequency adjustment. The stub tuning changes the resonance for 15 MHz per each mm stub length. The spacer tuning allows a wider tuning range of resonance by 256 MHz each mm of stub width, while it changes the gap length between the cathode and the aperture as well and might affect the beam focusing as a consequence (see Fig. 3).

The parameters which can be controlled for the operation of the triode cavity are following: The cathode emission  $J_c$  by means of the cathode temperature, the triode cathode cavity  $V_c$ , and the RF phase difference between triode cavity and main gun cavities  $\varphi$  by means of the input RF amplitude and phase control. Prior to testing the triode system we want to investigate suitable operational conditions which give optimal beam properties like emittance  $\epsilon_{r,n}$  and peak current  $I_{peak}$  for minimal power of back streaming electrons  $P_{back}$ .

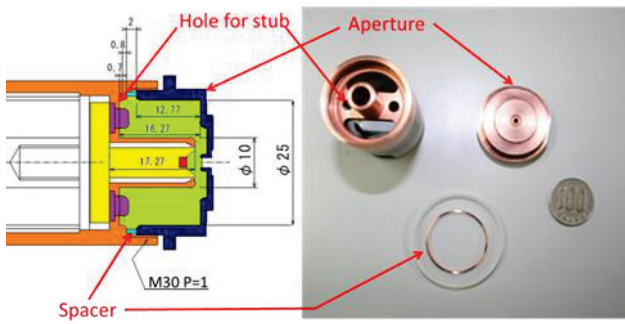


Figure 2: Photo of Triode cavity.

**PROCEDURE**

For numerical study we have used home developed particle tracking code KUBLAI [4], which includes the beam loading effect in calculation.

Figure 3 shows an eigenmode in the triode cavity used in this simulation. Since cylindrical symmetry is assumed, the effect of misalignment in the transverse position of the cathode was disregarded.

The designed operational parameters for triode type thermionic RF gun, which the design study of the triode cavity geometry was based on, are:  $V_c = 30$  kV,  $J_c = 80$  A/cm<sup>2</sup>, gap length  $L_g = 3.75$  mm (see Fig. 3) [5]. The cathode material is tungsten with 1mm diameter.

These conditions might have limitation in experimental feasibility. Especially, the supplied RF power for the triode gun may not be achievable at high values, that is why we study lower cavity voltage (see Table 1). Similarly, lower cathode current densities are studied than the designed value of 80 A/cm<sup>2</sup>. Another important operational parameter for the triode RF gun is the gap length  $L_g$ , since it might be changed by spacer for reasons of triode cavity resonance adjustment. Thus we investigate the beam performance for 2 different gap lengths  $L_g = 3.75, 3.35$  mm. These lengths correspond to the tuning range of triode cavity resonance of -100 MHz. This tuning range cannot be covered by stub system (the corresponded simulation has not been published yet).

Further we investigate the correlation between emission current density  $J_c$  and the peak current  $I_{peak}$  at the exit of triode RF gun. Thereby is important to determine the space charge limit, where the emission current can't be controlled by cathode temperature.

In Table 1 the parameters used for simulations are summarized. The values for beam charge and emittance at the RF gun exit were obtained from the electron energy distribution of  $\Delta E_k/E_k = 1\%$ .

For comparison Table 2 shows significant values of calculated beam properties for the 4.5 cell RF gun in conventional structure without the addition of the triode cavity.

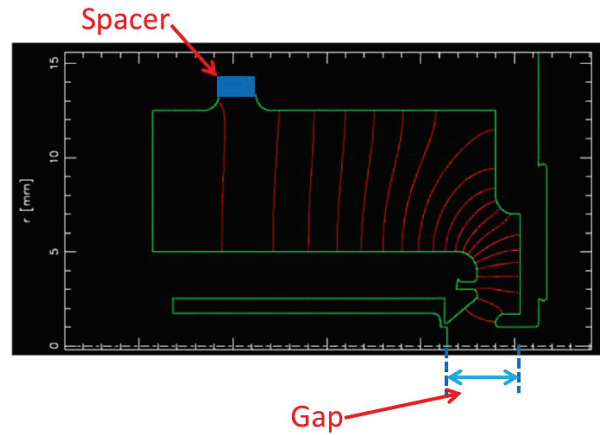


Figure 3: Eigenmode of triode cavity used in simulation.

Table 1: Input Parameters

	Triode	4.5cell
Cavity Voltage $V_c$	10, 20, 30 kV	11 MV
Gap Length $L_g$	3.35~3.75 mm	-
Current Density $J_c$	10~200 A/cm <sup>2</sup>	-

Table 2: Calculated Results (Conventional Type)

Total power of back-bombardment electrons $P_{back}$ [kW]	42.9
Peak Current $I_{peak}$ [A]	22
Normalized Transverse Emittance $\epsilon_{r,n}$ [ $\pi$ mm mrad]	1.23
Bunch Charge $Q$ [pC]	31

Under some conditions, the energy distribution was found to show two peaks. Figure 4 shows energy distribution and the peak current diagram according to the designed operational parameters of the triode RF gun. When such an energy distribution appears, we evaluated the beam parameters of the lower energy peak, because the peak current  $I_{peak}$  of the higher energy peak is found not to be high compared with the lower energy peak as shown in the right side graph in Figure 4.

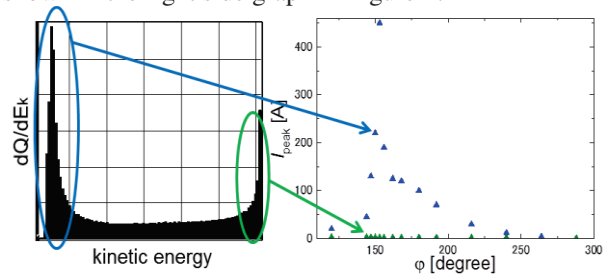


Figure 4: Energy distribution and the results of  $I_{peak}$  of triode RF gun ( $J_c = 80$  A/cm<sup>2</sup>,  $V_c = 30$  kV,  $L_g = 3.75$  mm).

**RESULTS AND DISCUSSIONS**

*Cavity Voltage*

Figure 5 shows dependence of  $P_{back}$  in the triode RF gun, normalized by the  $P_{back}$  in the conventional RF gun, on phase difference  $\phi$  and cavity voltage  $V_c$  ( $= 10, 20, 30$

kV). This diagram shows that in order to reduce more than 80% and 90% of  $P_{back}$ ,  $\phi$  was needed to be larger than 120 and 150 deg., respectively, for all the three cavity voltages. It can be also seen that there is no significant dependency of  $\phi$  with lowest  $P_{back}$  on  $V_c$ .

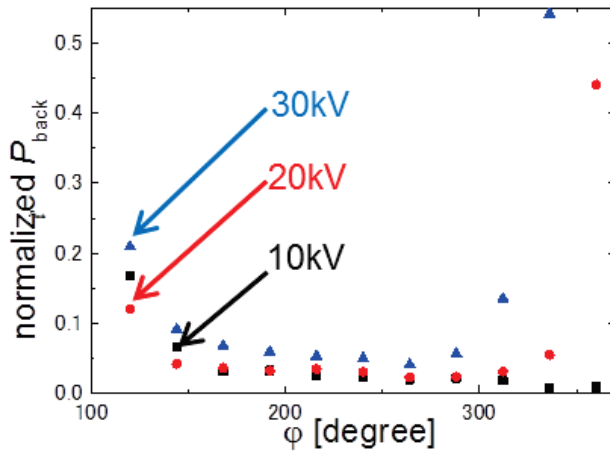


Figure 5: Dependence of  $P_{back}$  on  $\phi$  and  $V_c$  ( $J_c = 80$  A/cm<sup>2</sup>,  $L_g = 3.75$  mm).

Figure 6 shows the dependence of  $I_{peak}$  and bunch charge  $Q$  on  $\phi$  ( $\geq 120$  deg.) and  $V_c$ . From this calculation, it was found that acceptably high  $I_{peak}$  cannot be obtained for 10 kV. The degradation in  $I_{peak}$  is seen more significant than that in  $Q$ , and therefore may result from debunching effect because of the low cavity voltage. In constant, a high  $I_{peak}$  can be obtained at proper  $\phi$  for 20, 30 kV. Especially the 30 kV values with  $\phi$  around 153 deg. show  $I_{peak}$  of more than 400 A. Furthermore, we could confirm that  $\phi$  at the highest  $Q$  and  $I_{peak}$  increases as  $V_c$  becomes lower.

Figure 7 shows the dependence of normalized transverse emittance  $\epsilon_{r,n}$  on  $\phi$  ( $\geq 120$  deg.) and  $V_c$ . The results for 10 kV are not plotted because for 10 kV acceptable  $I_{peak}$  cannot be obtained. The  $\epsilon_{r,n}$  for 30 kV is better than that for 20 kV through almost all  $\phi$  except for around 150 deg. where  $\epsilon_{r,n}$  for 20 kV takes minimum. For 30 kV,  $\epsilon_{r,n}$  at  $\phi$  of 153 deg. is a bit higher than for 20 kV, but that is within the acceptable range. Further, it can be said that for either 20 kV and 30kV, by selecting the proper  $\phi$ , very high  $I_{peak}$  and comparatively low  $\epsilon_{r,n}$  are obtained as well as a low  $P_{back}$ .

Table 3 contains  $P_{back}$ ,  $I_{peak}$ ,  $Q$ ,  $\epsilon_{r,n}$ , at the proper  $\phi$  for 20 kV and 30 kV, respectively. The  $\phi$  which gives the highest  $I_{peak}$  is the desired  $\phi$  for the triode system, as the result of the most significant dependence of  $I_{peak}$  on  $\phi$ .

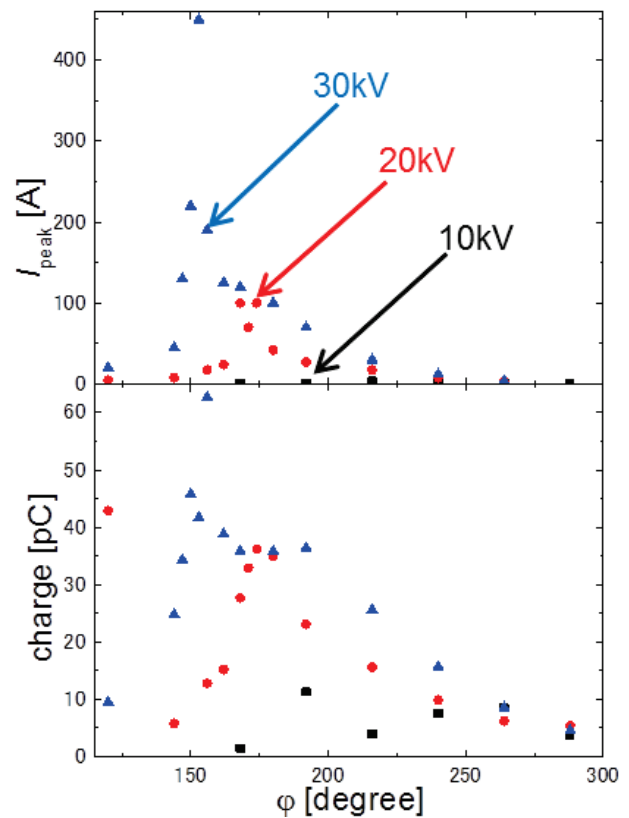


Figure 6: Dependence of  $I_{peak}$  and  $Q$  on  $\phi$  and  $V_c$  ( $J_c = 80$  A/cm<sup>2</sup>,  $L_g = 3.75$  mm).

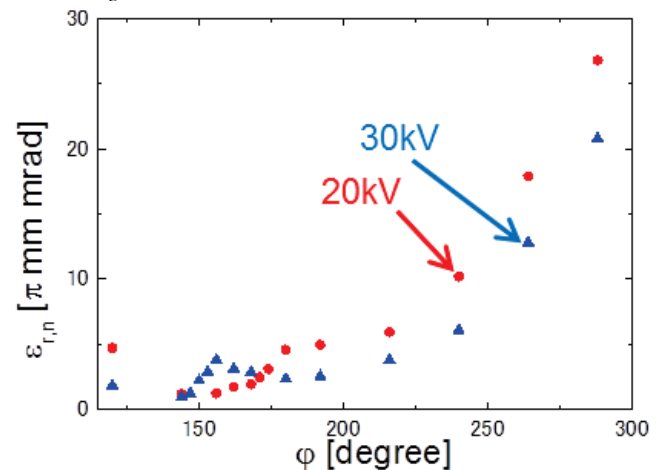


Figure 7: Dependence of  $\epsilon_{r,n}$  on  $\phi$  and  $V_c$  ( $J_c = 80$  A/cm<sup>2</sup>,  $L_g = 3.75$  mm).

2

Table 3: Results for Proper  $\phi$  ( $J_c = 80$  A/cm ,  $L_g = 3.75$  mm)

	20 kV	30 kV
$\phi$ [degree]	168	153
$P_{back}$ [kW]	1.54	3.51
$I_{peak}$ [A]	100	450
$Q$ [pC]	27.7	41.7
$\epsilon_{r,n}$ [ $\pi$ mm mrad]	1.92	2.87

### Gap Length

In the same way, we investigated the beam properties for another gap length of  $L_g = 3.35$  mm. Table 4 shows  $P_{back}$ ,  $I_{peak}$ ,  $Q$ ,  $\epsilon_{r,n}$  at the proper  $\phi$  of 20 kV and 30 kV in  $L_g = 3.35$  mm.

Table 4: Results for Proper  $\phi$  ( $J_c = 80$  A/cm<sup>2</sup>,  $L_g = 3.35$  mm)

	20 kV	30 kV
$\phi$ [degree]	156	137
$P_{back}$ [kW]	2.79	4.77
$I_{peak}$ [A]	110	400
$Q$ [pC]	46.6	52.7
$\epsilon_{r,n}$ [ $\pi$ mm mrad]	3.27	2.69

Compared with Table 3, the proper  $\phi$  is smaller for both cavity voltages. This is because the gap is shortened, so electrons reach the 1<sup>st</sup> cavity of 4.5 cell RF gun earlier. It is also found that similar beam properties could be obtained even if the gap length is changed.

### Current Density

Figure 8 shows the dependence of  $I_{peak}$  on  $\phi$  in the conditions:  $J_c = 30, 80$  A/cm<sup>2</sup>,  $V_c = 30$  kV,  $L_g = 3.75$  mm. It was found that the proper  $\phi$  for 30 A/cm<sup>2</sup> is around 153 deg. just like the proper  $\phi$  for  $J_c = 80$  A/cm<sup>2</sup>.

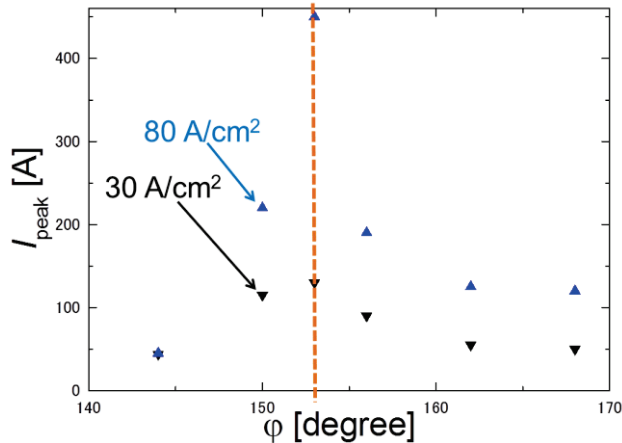


Figure 8: Dependence of  $I_{peak}$  on  $\phi$  ( $J_c = 30, 80$  A/cm<sup>2</sup>,  $V_c = 30$  kV,  $L_g = 3.75$  mm).

The dependence of  $I_{peak}$  on  $J_c$  at  $\phi = 153$  deg. is then studied and shown in Figure 9. Beam charge extracted on the cathode over an RF cycle is also shown in the figure as a function of  $J_c$ .

The space charge limit is determined from dependency of the extracted charge from the cathode on the  $J_c$ . The charge curve saturates around this limit of around 100 A/cm<sup>2</sup>. Until that point, cathode temperature is correlated with peak current. The  $I_{peak}$  increases almost linearly up to 100 A/cm<sup>2</sup> and decreases abruptly after that. However the  $I_{peak}$  curve extends the values of  $Q$  curve in the range  $J_c = 60-110$  A/cm<sup>2</sup>. This behaviour can be explained by the difference in integration process. For calculation of the  $Q$  the integration over whole RF period was done, whereas for  $I_{peak}$  the integration refers to the accelerating phase, which is a fraction of RF period. The abrupt decrease in

$I_{peak}$  at around 100 A/cm<sup>2</sup> may result from debunching and/or defocusing due to enhanced space charge effect. It is also found that  $I_{peak}$  exceeds 100 A that is 5 times higher than the conventional RF gun, even with a moderate  $J_c$  of 30 A/cm<sup>2</sup>.

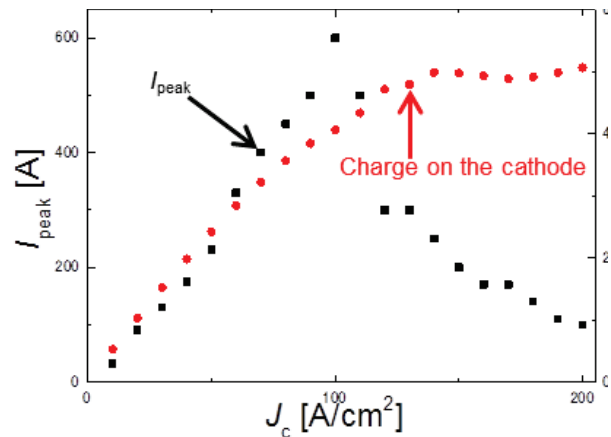


Figure 9: Dependence of  $I_{peak}$  and charge on the cathode on  $J_c$  ( $V_c = 30$  kV,  $\phi = 153$  deg.,  $L_g = 3.75$  mm).

### CONCLUSIONS

In this work we have numerically investigated beam performance of the triode type thermionic RF gun depending on operation parameters, namely the cavity voltage, gap length and emission current density from the cathode. As a result we found that the reduction of back-bombardment power can be achieved with lower cavity voltage of 20kV without significant losses in beam quality. Whereas for lower cavity voltage of 10 kV the peak current is too low. We expect that for higher cavity voltages the beam properties, especially the peak current, might be further improved. Moreover the change in the gap length of 0.4 mm does not significantly affect the beam properties.

Finally we could confirm that emission current is linearly correlated with peak current until the value of 100 A/cm<sup>2</sup> where space charge limit occurs.

### REFERENCES

- [1] K. Kanno, et al., "Design of Back-bombardment-less Thermionic RF gun", Japanese Journal of Applied Physics Vol. 41 Suppl. 41-1 (2002) 62-64
- [2] K. Masuda, et al., "Development of Thermionic Triode RF Gun", Proceedings of 31<sup>st</sup> International Free Electron Laser Conference, Liverpool, UK, Aug. 23-28, 2009
- [3] K Torgasin, et al., "Cold Test Of The Coaxial Cavity For Thermionic Triode Type RF Gun", Proceedings of IPAC2013, Shanghai, China, May. 12-17, 2013
- [4] K Masuda : Ph. D Thesis, Dept. of Engineering, Kyoto Univ(1998)
- [5] T. Shiyyama, et al., " A Triode - type Thermionic RF Gun For Drastic Reduction of Back-Streaming Electrons", Proceedings of FEL 2007, Novosibirsk, Russia, Aug. 26-31, 2007